

Barkhausen Noise as a Magnetic Nondestructive Testing Technique

Summary. In a large part of the hysteresis cycle of a ferromagnetic material, the magnetization process takes place through a random sequence of discontinuous movements of magnetic domain walls, giving rise to what is termed *magnetic Barkhausen noise* (MBN). This noise phenomenon can give information on the interaction between domain walls and stress configurations, or compositional microstructure. It is also a complementary nondestructive testing technique to eddy-current probe sensors as well as magnetic flux leakage (MFL), both established in the non-destructive evaluation industry.

This chapter takes a closer look at the influence of stress on magnetic domain configuration, and how this is reflected in the MBN signal. The latter can be analyzed by using a variety of parameters, and some of these are introduced during the discussion. Apart from domain configuration, stress also affects magnetic anisotropy which can reveal further details on the stress state present in the material. Concurrently, residual stresses and dislocations play a significant role in the MBN investigation, completing the analysis and adding to the competitiveness of MBN as a nondestructive testing technique for ferromagnetic materials.

2.1 Introduction

In a large part of the hysteresis cycle of a ferromagnetic material, the magnetization process takes place through a random sequence of discontinuous movements of magnetic domain walls, giving rise to what is termed *magnetic Barkhausen noise* (MBN) [1,2]. This noise phenomenon is investigated statistically through the detection of the random voltage observed on a pick up coil during the magnetization of the material [3]. Analysis of MBN can give information on the interaction between domain walls and stress configurations, or compositional microstructure [4]. It is also a complementary nondestructive testing technique to eddy-current probe sensors [5–7] as well as magnetic flux leakage (MFL) [8], both more established in the nondestructive evaluation industry.

2.2 A Basic Definition of Magnetic Barkhausen Noise

As mentioned above, during the action of a smoothly varying alternating magnetic field of intermediate intensity, abrupt irreversible changes in the form of MBN emissions (Fig. 2.1) are observed in the magnetization of a ferromagnetic material [3]. These irreversible changes occur in the steep part of the magnetization curve, and they account for magnetic hysteresis in ferromagnetic materials [9]. MBN is named after its discoverer [10], and is called “noise” due to the sound heard in the loudspeaker used in the original experiment. It is termed “magnetic” to distinguish it from *acoustic Barkhausen noise*, the latter being based on magnetoacoustic emission [11,12].

2.2.1 Types of MBN Experiments

There are two types of Barkhausen noise experiments that are usually performed. If the detection coil is placed on the surface of the specimen, the emissions are termed *surface Barkhausen noise*, whereas a coil wrapped around the specimen detects *encircling Barkhausen noise* [13,14] (Fig. 2.2). According to

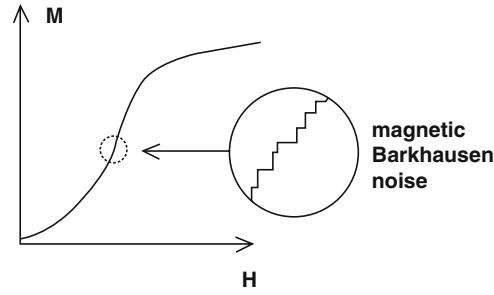


Fig. 2.1. Irreversible discontinuities in magnetization M as the ac magnetic field H is varied are termed magnetic Barkhausen noise

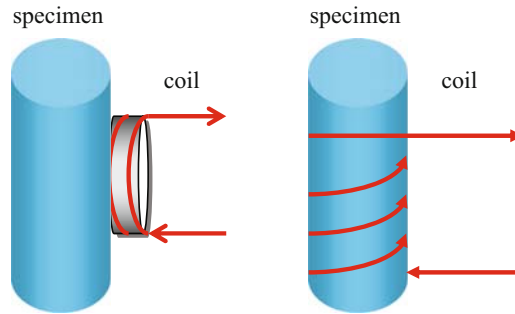


Fig. 2.2. Surface (*left*) vs. encircling (*right*) Barkhausen noise detection

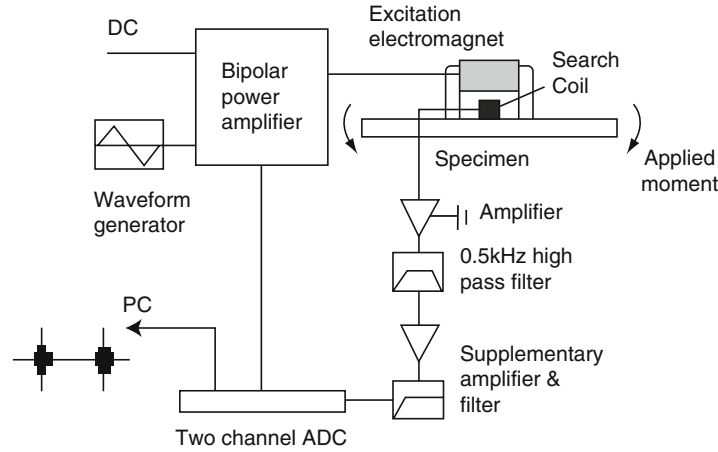


Fig. 2.3. A typical MBN measurement apparatus (reprinted from [16] (copyright 2004) with permission from Elsevier)

skin depth considerations [15], the estimated depth for minimum penetration of the magnetizing field is roughly 1 mm, whereas the depth from which the MBN signal originates is $\sim 30\mu\text{m}$. A typical MBN experimental setup [16] is sketched in Fig. 2.3. The MBN signal is detected by a search coil with a large number of turns of insulated copper wire wound around a ferrite cylinder. The output of the search coil is amplified and filtered [16].

2.2.2 Where does MBN Originate?

A ferromagnetic material that has not been magnetized consists of a large number of magnetic domains with random magnetic orientation, so that the bulk net magnetization is zero [3, 17] (Fig. 2.4). An external magnetic field tends to align the individual magnetic moments of the domains. Those domains with moments aligned most closely with the applied field will increase in volume at the expense of the other domains [9] (Fig. 2.5). The specimen becomes magnetized, as the walls move between adjacent domains [17].

When the external magnetic field is removed, the domains do not necessarily revert back to their original configuration [9]. This is because domain walls may have encountered pinning sites while moving, and to overcome these energy was expended [3, 9]. Once the wall has made it over the pinning site, there is no return path when the field is no longer acting. MBN is the irreversible “jump” of domain walls over local obstacles acting as pinning sites, such as grain boundaries, dislocations, inhomogeneities or other imperfections (Fig. 2.6). All lattice irregularities are likely to cause delays in domain wall movement, leading to uneven and discontinuous changes in magnetization [9, 18].

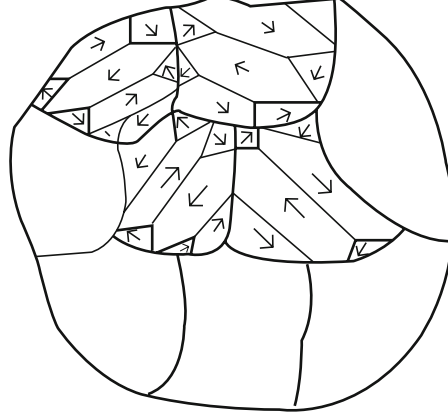


Fig. 2.4. Sketch of magnetic domains with random magnetic orientation in a polycrystalline ferromagnetic material, in the absence of an external magnetic field or stress. The *dark curves* represent grain boundaries (reprinted from [20])

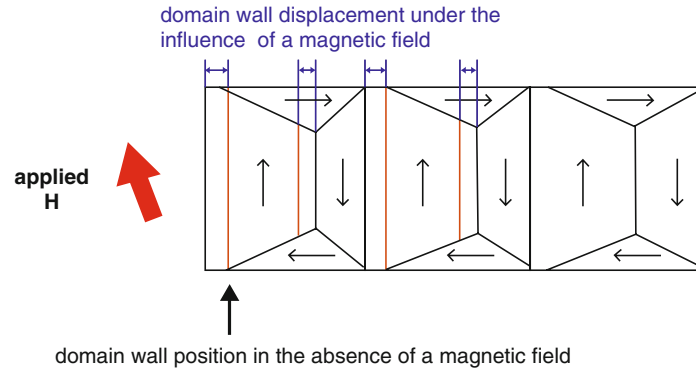


Fig. 2.5. Under the influence of an applied magnetic field, magnetic domains grow through wall displacement. Domains with moments aligned most closely with the applied field will increase in volume at the expense of the other domains. *Dashed lines* show wall positions in the absence of the field (reprinted from [20])

2.2.3 Formation of Magnetic Domains

Formation of magnetic domains occurs because of a minimization contest of the five basic energies involved in ferromagnetism:

$$E = E_{\text{exchange}} + E_{\text{magnetostatic}} + E_{\text{magnetocrystalline}} + E_{\text{magnetoelastic}} + E_{\text{wall}}. \quad (2.1)$$

The *exchange energy* E_{exchange} originates in quantum mechanical exchange forces or spin–spin interactions that are responsible for ferromagnetism [19]. A minimum in exchange energy is obtained when the spins of unpaired

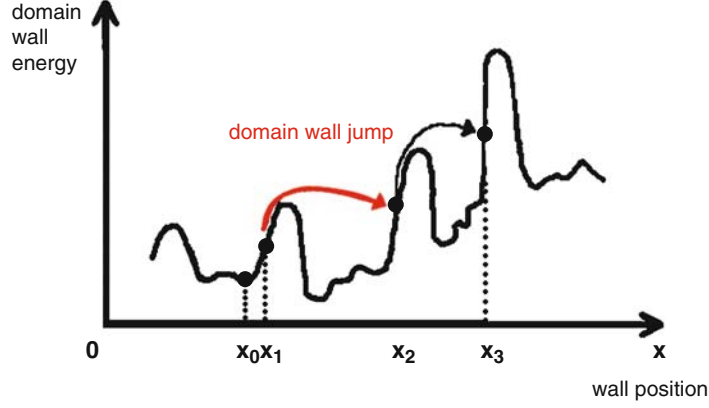


Fig. 2.6. Irreversible Barkhausen transitions. Domain walls overcome pinning sites and settle at energetically more favorable positions (reprinted from [20])

electrons are parallel, which is not possible in the same phase space. The *magnetostatic energy* $E_{\text{magnetostatic}}$ reaches a minimum when the magnetization of a magnetic domain is parallel to the external magnetic field [3, 9].

Crystal symmetry gives rise to a *magnetocrystalline (anisotropic) energy* $E_{\text{magnetocrystalline}}$ that becomes minimum when the magnetization of a magnetic domain is aligned with a preferred crystallographic direction, such as $\langle 100 \rangle$ in iron [15]. These directions are also termed *axes of easy magnetization* [3]. The crystal lattice strain is related to the direction of domain magnetization through the *magnetoelastic energy* $E_{\text{magnetoelastic}}$ [9]. It is a minimum when the lattice is deformed such that the domain is elongated or contracted in the direction of domain magnetization [9].

The fifth energy is related to the fact that domain walls have certain energy per unit area of surface and unit thickness of wall E_{wall} because atomic moments are not parallel to each other, or to an easy axis.

Increases and decreases in these five energies have consequences for the equilibrium of the crystalline lattice in the material such that not all energies can be minimum at the same time. Formation of a certain magnetic domain configuration is the outcome of the *sum* of the five basic energies being minimized, although the energies themselves may not be at their minimum [20].

2.2.4 MBN and 180° Domain Walls

Domain walls separating regions of opposite magnetic moment are called 180° walls, whereas walls lying at 90° to each other are appropriately termed 90° walls [3, 15]. Nickel has 109° and 71° domain walls [3, 15].

It is believed that MBN is primarily due to 180° domain wall motion [3, 9, 21]. The 90° domain walls have stress fields associated with them, as their magnetizations lie at right angles on either side of the wall, causing lattice

spacings to be slightly larger in the direction of magnetization. The resulting strain impedes with 90° domain wall motion, making them less competitive than 180° domain walls that have a higher velocity [22].

2.3 Stress Effects

Due to its high sensitivity to stress, MBN can be used as an independent nondestructive technique (NDT) for the evaluation of elastic stresses and strains [23], as well as plastic deformation and its consequences [20, 24].

2.3.1 Elastic Stress Causes Changes in Bulk Magnetization

A ferromagnetic material subjected to stress will cause changes to its bulk magnetization, even if no applied field is present [3]. This is because magnetic domains are influenced by stress and the resulting strain inside the material. Magnetic domains undergo stress-induced volume changes just like they would under an external magnetic field. As the internal elastic stress increases, the field required to move a domain wall across a pinning site, as well as the wall energy gradient increase, too [3]. The pinning sites themselves are also influenced by stress [25]. In fact, elastic strain effects are more influential on Barkhausen noise than plastic strain effects [25]. To gain a better idea of how stress influences MBN, a closer look at magnetic domains under the influence of stress is necessary.

2.3.2 Magnetic Domains Respond to Stress

An applied stress, just like an applied magnetic field, destroys the balance of the five energies. They have to readjust to minimize their sum [20]. If no external field is acting, the magnetostatic energy is zero. On the other hand, the magnetocrystalline and magnetoelastic energy are the dominant players [9, 15].

Under stress, both magnetocrystalline and magnetoelastic energy compete to determine the direction of the domain magnetization. Nevertheless, stresses in excess of 1,700 MPa are needed to counterbalance the effect of the magnetocrystalline energy, and change the direction of domain magnetization [26]. Therefore, the domain magnetization remains parallel to the *crystallographic* easy axis of the material, even under an applied stress.

Since realignment of magnetization with stress is not easily attained, the domain configuration minimizes its energy through movement of domain boundaries. A new energy configuration is achieved when domains lying closest to the direction of applied uniaxial tensile stress grow at the expense of domains with perpendicular domain magnetization. In contrast, under a compressive stress the domains with magnetic moments perpendicular to the axis of applied stress become energetically favorable [21]. In this manner, the magnetoelastic energy is decreased [15, 26].

There is another mechanism through which magnetic domains respond to an applied stress. In general under stress, there is an increase in the 180° domain wall population in the stress direction if the stress is tensile, with an opposite effect for compressive stress. Since MBN is associated with the pinning of magnetic domain walls, a higher signal is obtained along the direction of tensile stress, and a lower for compressive stress [27].

2.3.3 Magnetic Anisotropy and MBN

Magnetic properties of a material depend on the direction in which they are measured, and this phenomenon is known as *magnetic anisotropy* [3]. Only the magnetocrystalline anisotropy which is directly related to crystal symmetry is an intrinsic property of the material, while all other magnetic anisotropies are induced [15]. Quite often, design of commercial ferromagnetic materials is dependent on their magnetic anisotropy [23].

MBN is a suitable technique for detecting magnetic anisotropy in a ferromagnetic material, without regard to its origin. An MBN signal is detected at particular angles with respect to the specimen's axis, and after mathematical modeling it is plotted on a polar graph. The shape of the graph reveals the direction of the *magnetic easy axis* or magnetic anisotropy, because the MBN signal is large in that particular direction, as will be seen in subsequent sections.

2.3.4 Some Parameters Used in MBN Analysis

When modeling the MBN signal, two contributions are taken into account (1) that from domains responsible for an easy axis, also known as α and (2) a contribution from isotropically oriented domains represented by β [28]. The two contributions α and β are incorporated as fitting parameters into a mathematical expression describing a so-called $\text{MBN}_{\text{energy}}$

$$\text{MBN}_{\text{energy}} = \alpha \cos^2(\theta - \phi) + \beta, \quad (2.2)$$

where θ is the angle at which a magnetic field is applied, and ϕ is the easy axis direction [28]. The parameter α is obtained by subtracting β from the maximum " $\text{MBN}_{\text{energy}}$," due to β being a minimum in $\text{MBN}_{\text{energy}}$. α represents contributions from domains responsible for a magnetic easy axis, whereas β takes into account contributions from isotropically oriented domains [20]. The significance of the $\text{MBN}_{\text{energy}}$ is related to the change in magnetic flux under the influence of the magnetic field component parallel to a particular domain wall [20]. The latter will move if its coercivity is overcome by the field component parallel to the wall [28].

MBN measurements are taken at 10° intervals covering the entire 360° circle of an angular scan. The angle is with respect to the sweep field direction of the MBN sensor [20]. Equation (2.2) is fit to the measured MBN data, while

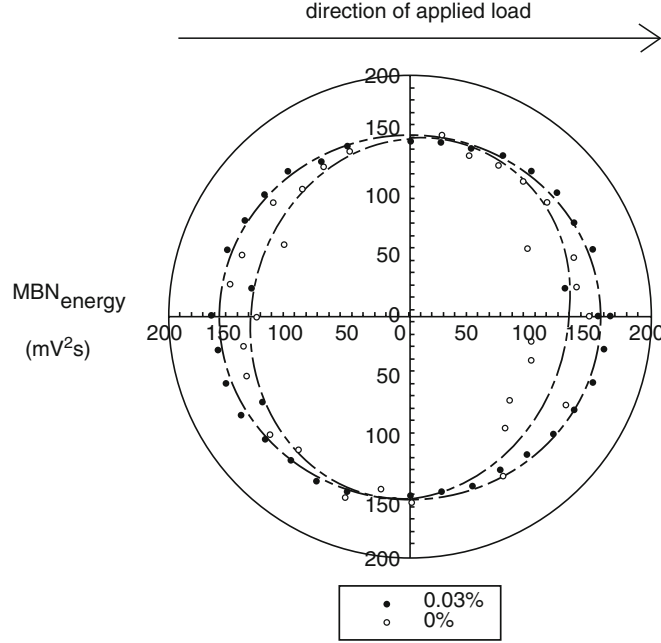


Fig. 2.7. Typical MBN_{energy} polar plot revealing a magnetic easy axis (or magnetic anisotropy) under the influence of an applied uniaxial tensile load. The plot is elongated in the direction of magnetic anisotropy which in the case of the 0.03% deformation is also the direction of the applied uniaxial tensile stress. The plot at 0% deformation is not a perfect circle, indicating that a magnetic anisotropy is present in the as is material due to prior processing which resulted in trapped residual stresses. The magnetic anisotropy of the as is material is in a direction different from the one along which the load will be subsequently applied (reprinted from [41])

the resulting calculated MBN_{energy} is plotted on a polar graph. Figure 2.7 shows a typical polar graph for the MBN_{energy} when magnetic anisotropy is present. In the absence of magnetic anisotropy, the MBN_{energy} plot is a perfect circle. If magnetic anisotropy is present such as for instance due to an applied uniaxial tensile load, the circle is elongated in the direction of the magnetic anisotropy which is also the direction of the uniaxial tensile load, transforming the plot from a circle into an ellipse [20].

Apart from MBN_{energy} , another parameter termed *pulse height distribution* is also used to characterize the MBN signal [20]. This is because the MBN signal consists of a collection of voltage pulses or “events” of varying amplitude that carry information about the magnetic state of the material. Usually, only voltage pulses above and below a certain threshold are considered in order to maintain integrity of the analysis. A positive slope between two consecutive measurements crossing the positive voltage threshold defines the onset of an event, while a similar positive slope crossing the negative voltage threshold defines the end of it.

The occurrence of events of different amplitude is represented in a graph termed a *pulse height distribution* where the absolute values of the event amplitudes are examined by height [20]. Actually, the $\text{MBN}_{\text{energy}}$ is obtained by calculating for each event the area between the time axis and the squared voltage pulse, and summing over all measured events.

2.3.5 Elastic Stress Influences on Magnetic Anisotropy

Angular MBN scans are very sensitive to stress-induced changes; therefore, they are a good indicator of the stress condition present in a ferromagnetic material at the time of the investigation. A large number of studies have conclusively demonstrated a high magnetic response in steel to applied elastic tensile or compressive stress, with an easy axis development along the direction of the tensile (Table 2.1a), and away from the compressive stress direction [27, 29–33].

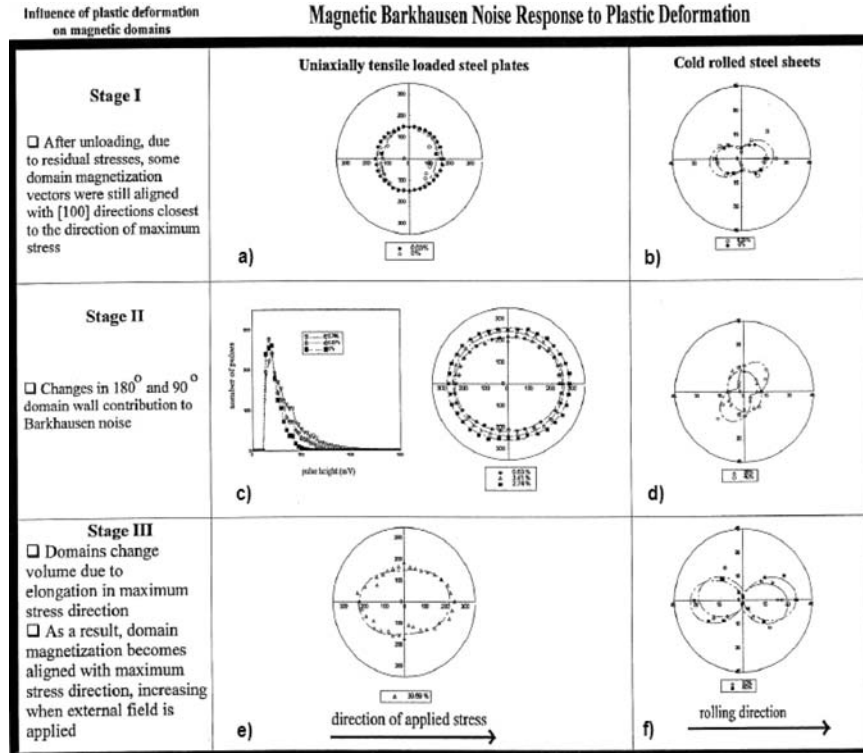
Domain magnetization vectors are aligned with [100] crystallographic directions closest to the direction of principal stress [20]. An applied elastic tensile stress increases $\text{MBN}_{\text{energy}}$ while creating a strong magnetic easy axis in the stress direction. The magnetic easy axis develops further with increased elastic stress, sometimes modifying its orientation while keeping up with directional variations in stress. Conversely, an applied compressive elastic stress decreases the $\text{MBN}_{\text{energy}}$ in the compression direction [34], and creates a magnetic easy axis perpendicular to applied stress [29]. A magnetic easy axis becomes even more pronounced with plastic deformation, while $\text{MBN}_{\text{energy}}$ values experience only a slight variation in the plastic regime, as opposed to the large increases observed during elastic deformation [25].

2.3.6 Plastic Deformation and Magnetic Anisotropy

A notable fact is that the magnetic easy axis continues to be present and become further pronounced in the plastic range of deformation [25] (Table 2.1c, e). Additionally, complex stress distributions left behind after mechanical processing such as cold rolling can also be characterized using MBN measured at different stages of rolling [20, 35] (Table 2.1b, d, f). Table 2.1 gives an overview of what can be detected using MBN, simultaneously showing some of the influence of elastic and plastic deformation on magnetic domains. The latter are best represented by changes in pulse height distributions, especially noticeable along directions of maximum shearing stress [20] (Table 2.1c, left).

Plastic deformation distorts the crystalline lattice permanently by *slipping* when the critical-resolved shear stress is reached on a slip plane. Between slipped and unslipped portions dislocations form that alter the interplanar spacing, creating strain fields and thereby volume changes in magnetic domains. While dislocation strain fields contribute to the redistribution of strain within a grain, they also alter the magnetic texture of the material.

Table 2.1. Elastic vs. plastic deformation effects on MBN_{energy} , pulse height distribution, as well as magnetic domains (a) A magnetic easy axis develops under an elastic stress, becoming more pronounced in (c) and (e) under plastic deformation. Changes in pulse height distribution become apparent in (c, left) at an angle of 45° with respect to the principal stress, along the direction of maximum shearing stress. Cold rolling reveals a complex stress distribution in (b), (d), and (f) [35]



Therefore, it is no surprise that plastic stress-induced effects are reflected in the measured MBN signal which depends so strongly on changes in magnetic domain configuration [25]. While elastic strain has been noticed to significantly alter the magnetic anisotropy α in the specimen, it has little influence on the isotropic background signal β . On the other hand, plastic deformation has the opposite effect, in as much as it changes β , but leaves α almost unaltered [25].

2.3.7 Effects of Residual Stresses

When using angular MBN scans to characterize samples that have reached the plastic regime and have been unloaded, it is noticed that the easy axis becomes less pronounced, nevertheless is still present [35]. Furthermore, interestingly the curve described by (2.2) does not fit experimental data. Higher

MBN_{energy} values are revealed in both axial and transverse directions to the previously applied tension, indicative of residual stresses trapped by plastic strains [20]. Residual stresses in welded T-section samples of SAE 1020 steel have been successfully detected in the past [13]. Significant increases in MBN signal have been observed in areas surrounding the weld before the sample underwent stress relief treatment. The latter involves annealing, a process known to reduce magnetoelastic energy [36].

Residual stresses are elastic in nature; however, they can be surrounded by nonuniform microstructural changes in the specimen [16]. This is because grains within a polycrystalline sample deform differently depending on their crystallographic orientation with respect to the direction of applied stress. While deforming, grains can lock in elastic intergranular stresses [37], and their influence is visible in the MBN signal [13, 25]. Figure 2.8 shows a correlation

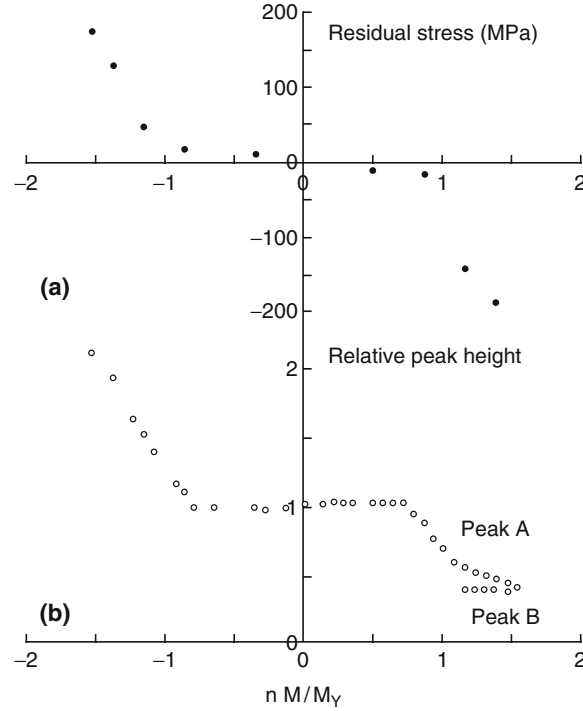


Fig. 2.8. Residual stress and relative MBN peak height in the unloaded state, correlated with the moment applied prior to unloading. (a) Residual stress determined by X-ray diffraction; (b) Normalized peak height from MBN profile. M/M_Y is the ratio between the maximum moment applied to a specimen before unloading, and the moment at which the stress reaches the yield point at the outer surface, while n is the sign of stress on the surface (positive for tension, and negative for compression) (reprinted from [16] (copyright 2004) with permission from Elsevier)

between residual stresses detected using X-ray diffraction and MBN peak height in unloaded specimens [16]. The same pattern is observed for both residual stresses and MBN peak height, proving that the two correlate very well.

2.3.8 Influence of Dislocations

Elastic stresses between grains adjust while dislocations appear in grain boundary regions [38], reducing stress concentration. Dislocations start to form even before the macroscopic elastic limit has been reached [39, 40]. The effect that dislocations have on the magnetic domain configuration can be witnessed through the abrupt and complex changes in $\text{MBN}_{\text{energy}}$ as well as pulse height distribution, changes characteristic of early stages of plastic deformation termed *microyielding* [40, 41]. The latter occurs as dislocation formation is initiated in some grains, while others remain intact [40].

The created strain fields result in increases in magnetic domains located in grain boundary regions. Their MBN signal is likely to be greater than the one of smaller size domains in the grain interior. A certain MBN response is obtained, dependent on how many grains develop dislocations. Not all grains undergo plastic deformation at the same time or at the same stress level. This is because of their different orientation with respect to the direction of applied stress. As deformation progresses reaching the *plastic stress regime*, massive dislocations are generated forming dislocation tangles as they move through the lattice. Also, more strain fields appear inside grains, as the bulk of the grain becomes affected by stress. New stress distributions emerge leaving their imprint on the MBN signal.

2.3.9 Selective Wall Energy Increases at Pinning Sites

Unequal size increases between magnetic domains, evidenced in the plastic stress regime, result in differences in the energetic level of domains. Furthermore, with enhanced dislocation density extending to more and more grains, domain wall energy gradient increases selectively at pinning sites [25]. Although single dislocations are too small to pin domain walls, dislocation tangles are believed to act as pinning sites to domain wall movement [42].

Figure 2.9 shows a possible domain wall energy redistribution at local pinning sites where walls experience a Barkhausen jump. When stress enters the plastic regime, some sites experience a significant energy increase, while simultaneously leaving other sites unchanged. Therefore, the Barkhausen transition is expected to occur from one high energy site to an even higher energy site, skipping sites with lower energy. Previous studies show that these unusual transitions are revealed in the detected MBN signal, in particular the pulse height distributions [20, 25].

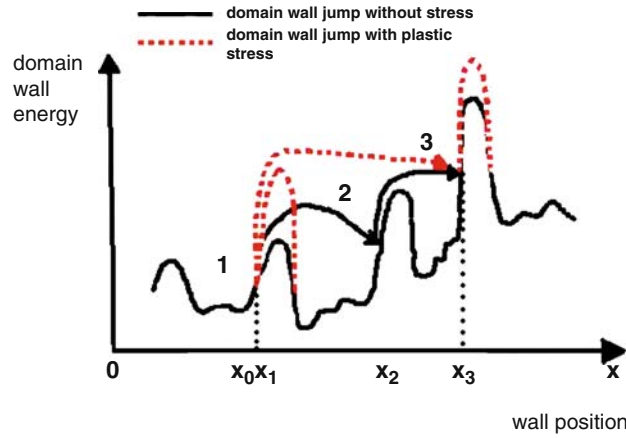


Fig. 2.9. Domain wall energy distribution at pinning sites with and without the influence of plastic stress. *Dashed lines* indicate changes that occur because of plastic stress, such as nonuniform increases in domain wall energy at some pinning sites and domain wall jumps that skip lower energy sites

2.3.10 Roll Magnetic Anisotropy

Variations in magnetic anisotropy are not only due to residual stresses or dislocations that alter magnetic domain configuration but also due to other factors such as crystallographic texture and various microstructural inhomogeneities [35,43]. These leave their imprint on MBN signals because they, too, determine domain wall dynamics.

MBN pulse height distributions are particularly indicative of such influences, as there are visible differences in their occurrence at various stages of plastic deformation. For instance, in the case of some typical nuclear reactor pressure vessel steel specimens subjected to varying levels of cold rolling, it was noticed that along the rolling direction the number of large MBN voltage pulses has diminished at reduction ratios of $\sim 25\%$, increasing again at $\sim 60\%$ reduction ratios [35].

These pulse height distribution observations correlate well with the detected variations in the magnetic anisotropy of the nuclear reactor pressure vessel steel specimens, as the preexisting anisotropy direction was destroyed at $\sim 25\%$ reduction ratio, increasing again and aligning with the rolling direction while deformation progressed to $\sim 60\%$ reduction ratio [35]. It is known that a $\{100\}(110)$ texture develops in severely deformed steel, detectable after 20–30% deformation [44], therefore crystallographic texture development is one of the reasons magnetic anisotropy experiences changes.

However, there is significant scatter about the “ideal” texture until higher levels of deformation (80–90%) are reached when texture formation is complete [44]. Nevertheless, texture cannot be the only factor responsible for roll induced changes in magnetic anisotropy, at least judging by the direction of the

latter displayed at different deformation levels. Stress levels are so high that inhomogeneous deformation is unavoidable, as internal elastic stresses become trapped in some parts of the material. These residual stresses, whether axially compressive due to the rolling process, or built up at grain boundaries or between crystallographic planes, bring their own contribution to the magnetic anisotropy of the cold rolled specimens.

The type of anisotropy described above is attributed to the cold rolling process itself, and has therefore been termed *roll magnetic anisotropy* [43,45,46]. It is believed to be due to complex metallurgical changes resulting in competing effects between crystallographic texture, as well as anisotropic microscopic and macroscopic residual stresses. In some cases, such as for nickel-cobalt alloys, a roll magnetic anisotropy has been observed along two directions, rather than a single one [46].

2.3.11 Limits in MBN Signal Increase with Plastic Stress

An applied stress that acts simultaneously on grains with different crystallographic orientations leads to longitudinal or shear incompatibility at grain boundaries [47]. The relative orientation of grains with respect to each other determines the type of incompatibility. Crystallographic orientations such as [100] and [111] experience longitudinal incompatibility [48], which means that one grain is in tension, while its neighbor is in compression. The stress at grain boundaries induced by longitudinal incompatibility is almost three times higher than the critical-resolved shear stress within a grain [49]. Therefore, dislocations are more likely generated at grain boundaries before they can form in the interior of the grain. Also, the interplanar spacing is altered in the vicinity of the actual dislocation, giving rise to what is termed *strain field of the dislocation* [47].

The formation of these dislocation induced strain fields results in local variations in interplanar distance along a certain crystallographic direction within a grain. Nevertheless, these can only accommodate so much elastic strain before slip systems are activated and plastic flow initiates, leading to work hardening. The latter will increase slightly the threshold for plastic flow, allowing some elastic strain to continue to build up, but this build up will eventually reach its limits. Mughrabi [50] advanced the idea of hard mechanical regions consisting of dislocation tangles in and near grain boundaries, surrounded by a softer matrix. The hard regions are built of small volumes assumed to be under tensile stress, while separated by larger volumes (soft regions) under compressive stress [50].

Thus, plastic deformation introduces permanent lattice distortion with different consequences for each particular domain configuration. Irregular stress distributions affect the volume of magnetic domains, especially for those in grain boundary regions that experience increases in volume before their neighbors in the grain interior. But every magnetic domain size modification implies wall movement, hence variations in MBN signal. Nevertheless, these

volume changes can only extend so far, as the resulting additional strain fields attributed to massive plastic deformation will ultimately put restrictions in domain size increase, as well as impede the simultaneous motion of domain walls. These limitations lead to a slow down in MBN signal increase, fact evidenced in measurements performed at very high levels of deformation that show only a small rise in signal [41]. Some authors consider this effect a “magnetic degradation” [51, 52].

2.4 Effects of Microstructure on MBN

2.4.1 Variations in Grain Size

Bertotti et al. [53] investigated the effect of grain size on MBN, observing that the boundaries of grains are likely sources for domain wall pinning. Ng et al. [54] confirmed that a large number of grain boundaries result in more intense Barkhausen noise emissions. The large number of boundaries is found in samples with smaller grains that have been annealed at lower temperatures. Small grain samples have larger MBN signals because the boundaries act as pinning sites, and since their fractional volume is larger, more pinning sites need to be overcome when the walls move.

Krause et al. [27] suggested that the number of 180° domain walls increases in the presence of applied tensile stress, and derived an expression for the change in magnetoelastic energy under these circumstances. From this expression, they calculated a threshold stress that would be necessary to add another domain wall to the configuration. This threshold stress depends on the grain size and it increases with the number of existing domain walls. Hence, MBN activity is strongly linked to grain size and grain boundaries.

Ng et al. [54] advanced the idea that the interaction between the domain walls and dislocation tangles leads to different MBN profiles than the interaction between the walls and grain boundaries. They used this argument to explain secondary peaks observed in some of the MBN signals. This is because the physical nature of the pin is assumed to dictate the restoring force acting on the wall.

Grain size influences the number of defects in the specimen and hence its magnetic properties [55]. Ranjan et al. [56] substantiated these findings by showing that the number of MBN pulses varies inversely with grain size in annealed nickel. Large number of pulses means smaller grains, therefore more pinning sites, and possibly more defects.

Gatelier-Rothea et al. [57] reported a decrease in MBN signal when the grain size in iron samples increased. That grain size is inversely proportional to the detected MBN signal was also noticed by Tiito et al. [58] who investigated the magnetic behavior of steel specimens of varying grain size. However, precipitates and segregation of phosphorus at grain boundaries can act as additional pinning sites for domain walls, increasing the number of MBN pulses even in large grained specimens, as observed experimentally in decarburized steel [56].

2.4.2 Compositional and Phase Influences

Compositional variations can bring their own contribution to signals, rendering the MBN analysis more complicated. Plain carbon steels were studied by Kameda et al. [59], who found that variations in MBN signal are obtained because of phase changes such as carbide precipitation or intergranular impurity segregation left behind after heat treatment. Jiles [60] investigated plain carbon steels of the AISI 10xx series, documenting how MBN changes with carbon content due to increased pinning of domain walls by carbide particles. When the latter built networks of lamella carbide, they provided stronger pinning, as opposed to the spheroidized carbides that impeded less the movement of domain walls. Heat treatment of carbon steel AISI 4130 produces pearlite, bainite, and martensite, each with its distinct MBN signature [60].

Blaow et al. [61] compared MBN signal profiles in cementite, pearlite, and martensite specimens with and without compressive strain. When the specimens were undeformed, MBN signals were more pronounced in the magnetically soft spheroidized cementite, however reduced in pearlite or the magnetically hard martensite specimen tempered at 400°C. The latter also displayed multiple MBN peaks with strain, whereas pearlite and a martensite specimen tempered at 180°C showed only a single peak. However, that peak increased systematically with strain. It should be noted that the MBN parameters employed in these studies are quite different from the ones described above in earlier sections. Instead, magnetization curves were recorded, and it is on these curves that one or more peaks were noticed.

The most significant change with strain in MBN signal profiles in the Blaow et al. [61] study was observed in the spheroidized cementite specimens. A single peak in the undeformed state was followed by peak broadening with three overlapping peaks. It is assumed that cementite lamellas provide strong directional pinning to domain wall motion, as previous reports indicate [62,63]. All MBN signal changes were reversible when loads were removed while still in the elastic stage of deformation [61].

2.4.3 MBN Behavior in Different Materials

Three peak MBN profiles were also observed in the magnetization curves of unstrained mild steel [64] and were attributed to spike (or residual) domains. These are usually nucleated and annihilated in the knee region of the hysteresis loop, but some are retained in the specimen upon saturation. Because some spike domains are retained, reversal of the field causes abrupt nucleation of new domains when the knee region is reached again [64]. Around saturation, the incomplete annihilation of these spike domains causes some MBN activity, as Ng et al. [54] pointed out when they observed a second peak at higher fields in the magnetization curve of low carbon steel.

Buttle et al. [65] investigated the magnetization of quite different material types and observed a single peak in a cold-worked Ni sample, however noticed

a three peak MBN profile in an Fe sample. Interestingly, Thompson et al. [66] and Lo et al. [67] reported double peak MBN signals in ferritic-pearlitic steel with higher volume fraction. A second peak in the MBN signal was also noticed by Kleber et al. [68] who applied a compressive elastic and later plastic stress to mild steel as well as Armco iron specimens. Nevertheless, Armco iron displayed different MBN behavior than mild steel.

In the experiment of Kleber et al. [68] an increase in MBN signal was detected with tensile as well as compressive plastic stress in Armco iron specimens [68]. The magnetic behavior seen in Armco iron was ascribed to dislocation tangles and their interaction with magnetic domain walls [68]. On the other hand, mild steel displayed a decrease in MBN with tensile plastic stress, and almost no change in compression, contrary to earlier reports by other groups [25].

Kleber et al. [68] concluded that residual internal stresses play a different role in influencing MBN behavior in tensile vs. compressive deformation in mild steel. By this argument, they attributed the changes in MBN observed in the mild steel specimens to residual stresses. In contrast, dislocation effects on MBN were assumed to be independent of the sign of plastic strain. Nevertheless, the overall objective of the Kleber et al. study [68] was to separate the effect of dislocations from that of residual internal stresses in the plastic regime, hence two materials with different yield strengths were chosen.

A somewhat related goal was targeted by Moorthy et al. [69] in their work on the effects of fatigue and overstressing on the MBN response of case-carburized En36 steel. Given the type of steel and its mechanical processing, these specimens had a sharp change in microhardness with depth level, so that a crack initiated at the surface propagated very fast into the material. Furthermore, dislocations had a small chance to form prior to crack formation, as smaller stress levels did not allow dislocation initiation, while crack formation preceded larger stresses necessary for developing dislocations. Of course, the magnetic behavior was observed to also vary under these circumstances.

In Moorthy et al.'s study [69], MBN peak height increased in the vicinity of the crack, hence this technique was able to detect the crack location. Nevertheless, crack growth represented only a small fraction in the fatigue life of the case-carburized steel, with specimens failing soon after crack initiation. On the other hand, detection of residual stresses proved to be a more useful indicator of impending failure, since the MBN technique was able to better assess the maximum level of bending stress prior to crack initiation. Alerting users before cracks have a chance to form is definitely a more favorable alternative to finding out that the component is about to fail as soon as a crack is detected [69].

The MBN response of nonoriented (3 wt.%) Si-Fe was investigated by V.E. Iordache et al. [70] who subjected the steel specimens to uniaxial tensile stress beyond the macroscopic elastic limit, unloaded the specimens, and performed MBN measurements again during a second reloading. The study allowed a comparison of the different aspects of tensile deformation, from elastic strain

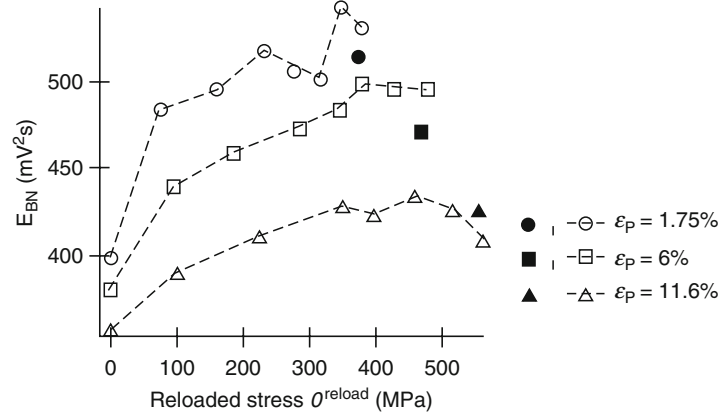


Fig. 2.10. Barkhausen noise energy vs. reloaded stresses (*open marks*) compared with values under initial applied stress (*full marks*) for three nonoriented (3 wt.%) Si-Fe specimens (reprinted from [51] (copyright 2003) with permission from Elsevier)

to microyielding, plastic yielding, and strain hardening. The measurements performed in situ during reloading (Fig. 2.10) revealed some similarities to previous studies of the magnetic behavior of steel, even though the latter were not performed after loading for a second time [20,25]. It should be noted that loading, unloading, and reloading again increases MBN values measured at the same level of stress as during the first loading [71].

2.5 Competitiveness of MBN in Nondestructive Evaluation

2.5.1 Usefulness of MBN for MFL

MFL is an effective inspection method for evaluating corrosion and defect impact on pipelines while they are still in service [72]. It is based on inducing a magnetic flux into the walls of a pipeline, using strong permanent magnets. The flux will “leak out” if metal loss exists, such as when the walls contain defects. A Hall sensor detects the leaking flux that depends on defect geometry, as well as any associated stresses [73]. Given the complexity of the factors influencing the MFL signal, MBN can be of assistance in giving a correct interpretation, provided results from both techniques are compared to establish a common pattern under similar circumstances [73].

Quite often, simulation tools relying on finite element analysis have been employed to model magnetic flux patterns around corrosion defects [74]. Results from MFL studies [73] indicate that flux signals around the defect, in particular dents, are sensitive to elastic residual stresses, but not to plastic deformation. This is in agreement with MBN studies on elastic vs. plastic

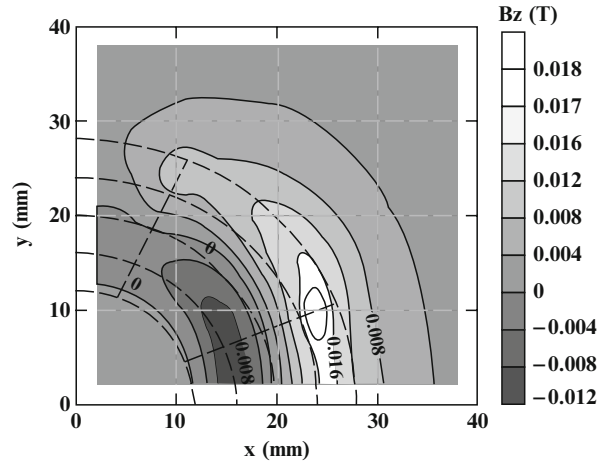


Fig. 2.11. Simulated MFL contour maps obtained 0.5 mm underneath a dented steel plate. The maps show the combined effect of dent geometry and stresses (reprinted from [75] (copyright 2005) with permission from Elsevier)

deformation effects, which also indicate that elastic stress has a more pronounced influence on magnetic behavior than plastic stress [20,25].

A recent MFL study [73] revealed that the radial signal is most determined by compressive stress configurations perpendicular to the flux path, lowering steel permeability and forcing flux out of the pipe [73]. Figure 2.11 shows the simulated magnetic field contour maps on the bottom side of a steel plate containing a dent, illustrating the effect of both dent geometry and stress configurations on the MFL signal. It seems that geometry is the dominant factor, and not stress distributions around the dent, except for a very pronounced peak in the lower part of the figure. The peak is attributed to stress and correlates well with previous findings of MBN studies [20,25,75].

The MFL simulation results [73] were correlated with experimental magnetic flux patterns determined using the MFL technique. Specimens were subjected to a residual stress removal treatment before a dent was applied, to ensure that only stress configurations associated with the dent itself were present. Experimental results matched very closely those obtained by simulation [73]. The knowledge gained through prior MBN studies on stress configurations and magnetic behavior assisted in obtaining a more complete interpretation of MFL signals [73].

2.5.2 Need for Calibration of MBN as NDT

The main advantage of magnetic Barkhausen noise as a nondestructive technique is that it reveals complex changes in materials structure that originate in microstructural properties, as well as stress configurations, together

leaving their imprint on the material. How the latter responds depends on multiple factors, each with a specific influence on magnetic behavior. Nevertheless, these factors are difficult to dissociate and treat individually, requiring an experienced user to give the appropriate interpretation to the measured MBN data.

For instance, magnetic domains of neighboring grains of the same crystallographic orientation could become simultaneously active. In this case, an enhanced MBN signal is likely to be obtained, however this large signal may not be entirely because of crystallographic texture. Furthermore, reorientation of grains that can occur with plastic deformation is likely to cause redistribution of internal stresses, potentially destroying the effects of other factors such as residual stresses. Fortunately, crystallographic reorientation only happens at high deformation levels, usually associated with mechanical processing [44].

User knowledge and experience are extremely important in MBN data analysis. Nevertheless, because MBN depends on so many influential variables, it is still necessary to resort to comparative studies, and ultimately calibrate measurements. An undeformed specimen or a known microstructural state needs to act as a standard for a particular type of alloy. In spite of commonalities, one should not directly compare MBN results for different types of plain carbon steels. Their prior magnetic history, processing treatment and ultimately type of steel will determine their MBN response.

References

1. R.M. Bozorth, *Ferromagnetism* (IEEE Press, New York, 1951)
2. W.A. Theiner, H.H. Williams, Determination of Microstructural Parameters by Magnetic and Ultrasonic Quantitative NDE, in *Nondestructive Methods Material Property Determination* (Plenum Press, New York, 1984), p. 249
3. S. Chikazumi, *Physics of Magnetism* (Wiley, New York, 1964)
4. V.N. Shah, P.E. MacDonald, *Residual Life Assessment of Major Light Water Reactor Components*, vol. 1 (Idaho National Engineering Laboratory, Seattle, 1987), p. 144
5. S. Nath, B. Wincheski, J.P. Fulton, M. Namkung, *IEEE Trans. Magn.* **30**(6), 4644 (1994)
6. R.A. Wincheski, M. Namkung, *Aerospace Am.* **36**(3), 27 (1998)
7. B. Wincheski, J.P. Fulton, S. Nath, M. Namkung, J.W. Simpson, *Mat. Eval.* **52**(1), 22 (1994)
8. V. Babbar, B. Shiari, L. Clapham, *IEEE Trans. Mag.* **40**(1), 43 (2004)
9. R. Becker, W. Döring, *Ferromagnetismus* (Springer Verlag, Berlin, 1939)
10. H. Barkhausen, *Physik. Z.* **20**, 401 (1919)
11. A.E. Lord, in *Acoustic Emission*, ed. by W.P. Mason, R.N. Thurston. *Physics Acoustics*, vol. 9 (Academic Press, New York, 1975)
12. M. Namkung, S.G. Allison, J.S. Heyman, *IEEE Trans. Ultrasonics Ferroelectrics Freq. Control* **33**(1), 108 (1986)
13. K. Tiito, in *Nondestructive Evaluation: Application to Materials Processing*, ed. by O. Buck, S.M. Wolf (ASM, Materials Park, Ohio, 1984), p. 161

14. X. Kleber, A. Vincent, *NDT&E Int.* **37**, 439 (2004)
15. B.D. Cullity, *Introduction to Magnetic Materials*, 2nd edn. (Addison-Wesley, New York, 1972)
16. M. Blaow, J.T. Evans, B. Shaw, *Mater. Sci. Eng.* **A386**, 74 (2004)
17. D.C. Jiles, *Introduction to Magnetism and Magnetic Materials* (Chapman and Hall, New York, 1991)
18. J.C. McClure, Jr., K. Schröder, *CRC Crit. Rev. Solid State Sci.* **6**, 45 (1976)
19. W. Heisenberg, *Z. Physik* **49**, 619 (1928)
20. C-G. Stefanita, Ph.D. Thesis, Department of Physics, Queen's University, Kingston, Ontario, Canada, 1999
21. D. Utrata, M. Namkung, *Rev. Progr. Quant. Nondestr. Eval.* **2**, 1585 (1987)
22. R.S. Tebble, *Proc. Phys. Soc. Lond. B* **68**, 1017 (1955)
23. J-K. Yi, *Nondestructive Evaluation of Degraded Structural Materials by Micro-magnetic Technique*, Ph.D. Thesis, Department of Nuclear Engineering, Korea Advanced Institute of Science and Technology, Taejon, Korea (1993)
24. H. Kwun, G.I. Burkhardt, *Electromagnetic Techniques for Residual Stress Measurement*, 9th edn. *Metals Handbook*, vol. 17 (ASM International, Materials Park, 1989), p. 159
25. C-G. Stefanita, D.L. Atherton, L. Clapham, *Acta Mater.* **48**, 3545 (2000)
26. C. Kittel, J.K. Galt, *Solid State Phys.* **3**, 437 (1956)
27. T.W. Krause, L. Clapham, A. Pattantyus, D.L. Atherton, *J. Appl. Phys.* **79**(8), 4242 (1996)
28. T.W. Krause, L. Clapham, D.L. Atherton, *J. Appl. Phys.* **75**(12), 7983 (1994)
29. C. Jagadish, L. Clapham, D.L. Atherton, *IEEE Trans. Magn.* **25**(5), 3452 (1989)
30. C. Jagadish, L. Clapham, D.L. Atherton, *NDT Int.* **22**(5), 297 (1989)
31. C. Jagadish, L. Clapham, D.L. Atherton, *J. Phys. D: Appl. Phys.* **23**, 443 (1990)
32. C. Jagadish, L. Clapham, D.L. Atherton, *IEEE Trans. Magn.* **26**(1), 262 (1990)
33. T.W. Krause, K. Mandal, C. Hauge, P. Weyman, B. Sijgers, D.L. Atherton, *J. Magn. Magn. Mater.* **169**, 207 (1997)
34. H. Kwun, G.L. Burkhardt, *NDT Int.* **20**, 167 (1987)
35. C-G. Stefanita, L. Clapham, J.-K. Yi, D.L. Atherton, *J. Mater. Sci.* **36**, 2795 (2001)
36. R.L. Pasley, *Mater. Eval.* **28**, 157 (1970)
37. L.E. Murr, *Met. Trans.* **6A**, 427 (1975)
38. K. Tangri, T. Malis, *Surface Sci.* **31**, 101 (1972)
39. R.M. Douthwaite, T. Evans, *Acta Met.* **21**, 525 (1973)
40. V. Moorthy, S. Vaidyanathan, T. Jayakumar, B. Raj, B.P. Kashyap, *Acta Mater.* **47**, 1869 (1999)
41. C-G. Stefanita, L. Clapham, D.L. Atherton, *J. Mater. Sci.* **35**, 2675 (2000)
42. A.J. Birkett, W.D. Corner, B.K. Tanner, S.M. Thompson, *J. Phys. D: Appl. Phys.* **22**, 1240 (1989)
43. W. Six, J.I. Snoek, W.G. Burgers, *De Ingenier* **49E**, 195 (1934)
44. G.E. Dieter, *Mechanical Metallurgy* (McGraw Hill, New York, 1961)
45. S. Chikazumi, K. Suzuki, H. Iwata, *J. Phys. Soc. Jpn.* **15**(2), 250 (1960)
46. N. Tamagawa, Y. Nakagawa, S. Chikazumi, *J. Phys. Soc. Jpn.* **17**(8), 1256 (1962)
47. J.P. Hirth, *Met. Trans.* **3**, 3047 (1972)
48. M.A. Meyers, K.K. Chawla, *Mechanical Metallurgy: Principles and Applications* (Prentice Hall, New Jersey, 1984)
49. M.A. Meyers, E. Ashworth, *Phil. Mag. A* **46**(5), 737 (1982)

50. H. Mughrabi, *Acta Metall. Mater.* **31**, 1367 (1983)
51. V.E. Iordache, E. Hug, N. Buiro, *Mater. Sci. Eng.* **A359**, 62 (2003)
52. K. Kashiwaya, *Jpn. J. Appl. Phys.* **31**, 237 (1992)
53. G. Bertotti, F. Fiorillo, A. Montorsi, *J. Appl. Phys.* **67**(9), 5574 (1990)
54. D.H.L. Ng, K.S. Cho, M.L. Wong, S.L.I. Chan, X-Y. Ma, C.C.H. Lo, *Mat. Sci. Eng.* **A358**, 186 (2003)
55. H. Sakamoto, M. Okada, M. Homma, *IEEE Trans. Magn.* **23**, 2236 (1987)
56. R. Ranjan, D.C. Jiles, O. Buck, R.B. Thompson, *J. Appl. Phys.* **61**(8), 3199 (1987)
57. C. Gatelier-Rothea, J. Chicois, R. Fougères, P. Fleischmann, *Acta Mater.* **46**, 4873 (1998)
58. S. Tiito, M. Ojala, S. Säynäjäkangas, *NDT Int.* **9**, 117 (1976)
59. J. Kameda, R. Ranjan, *Acta Metall.* **35**, 1515 (1987)
60. D.C. Jiles, *J. Phys. D* **21**, 1186 (1988)
61. M. Blaow, J.T. Evans, B.A. Shaw, *Acta Mater.* **53**, 279 (2005)
62. M.G. Hetherington, J.P. Jakubovics, J. Szpunar, B.K. Tanner, *Philos. Mag. B* **56**, 561 (1987)
63. L.J. Dijkstra, C. Wert, *Phys. Rev.* **79**, 979 (1950)
64. D.G. Hwang, H.C. Kim, *J. Phys. D: Appl. Phys.* **21**, 1807 (1988)
65. D.J. Buttle, C.B. Scruby, J.P. Jakubovics, C.A.D. Briggs, *Philos. Mag. A* **55**, 717 (1986)
66. S.M. Thompson, B.K. Tanner, *J. Magn. Magn. Mater.* **123**, 283 (1993)
67. C.C.H. Lo, C.B. Scruby, *J. Appl. Phys.* **85**, 5193 (1999)
68. X. Kleber, A. Vincent, *NDT&E Int.* **37**, 439 (2004)
69. V. Moorthy, B.A. Shaw, P. Hopkins, *NDT&E Int.* **38**, 159 (2005)
70. V.E. Iordache, E. Hug, N. Buiro, *Mater. Sci. Eng.* **A359**, 62 (2003)
71. M. Lindgren, T. Lepistö, *NDT&E Int.* **34**, 337 (2001)
72. W. Mao, C. Mandache, L. Clapham, D.L. Atherton, *Insight* **43**(10), 688 (2001)
73. V. Babbar, L. Clapham, *J. Nondestruct. Eval.* **22**(4), 117 (2003)
74. N. Ida, W. Lord, *IEEE Trans. Magn.* **19**(5), 2260 (1983)
75. V. Babbar, J. Bryne, L. Clapham, *NDT&E Int.* **38**, 471 (2005)

From Bulk to Nano

The Many Sides of Magnetism

Stefanita, C.-G.

2008, XX, 174 p., Hardcover

ISBN: 978-3-540-70547-5